INDIAN JOURNAL OF SCIENCE AND TECHNOLOGY

RESEARCH ARTICLE

Vulnerability assessment of hydrogeologic units in parts of Enugu North, Southeastern Nigeria, using integrated electrical resistivity methods

Mirianrita Ngozi Ossai[1]*, Francisca Nneka Okeke[1], Daniel Nnaemeka Obiora[1], Johnson Cletus Ibuot[1]

1 Department of Physics and Astronomy, University of Nigeria, Nsukka, Enugu State, Nigeria

OPEN ACCESS

Received: 20-08-2020

Accepted: 05-09-2020

Published: 15-09-2020

Editor: Dr. Natarajan Gajendran

Citation: Ossai MN, Okeke FN, Obiora DN, Ibuot JC (2020) Vulnerability assessment of hydrogeologic units in parts of Enugu North, Southeastern Nigeria, using integrated electrical resistivity methods. Indian Journal of Science and Technology 13(34): 3495-3509. https://doi.org/10.17485/IJST/v13i34.1366

***Corresponding author**.

rita.ossai@unn.edu.ng

Funding: None

Competing Interests: None

Published By Indian Society for Education and Environment (iSee)

ISSN
Print: 0974-6846
Electronic: 0974-5645

Abstract

Aim/objectives: This research is geared towards integrating Vertical Electrical Soundings (VES) and Electrical Resistivity Tomography (ERT) profiles constrained with geoelectric sections and borehole logs to assess the vulnerability of the aquifer units employing Aquifer Vulnerability Indexing (AVI) method. **Method**: The dataset used in this study comprises of fifty VES, five ERT profiles surveyed in parts of Enugu north in Enugu state, two geoelectric sections and three borehole logs. The computer and manual interpretation of VES resistivity data using WinResist software gave values of resistivity, depth and thickness of each geoelectric layer using half current electrode spacing of 1.0 to 450.0 m and maximum current electrode spacing of 900 m. 2D imaging data from the measured field resistance values were processed using RES2DINV×32 version 3.71.115 software. The geoelectrical sections show the variation of resistivities with depth along transcent lines. The geohydraulic parameters were also estimated. **Finding**: Interpreted VES data revealed five to six geoelectric layers and fundamental parameters generated were used to estimate the values of hydraulic conductivity (σ) and hydraulic resistance (C) of the covering layers ranging from 0.010 to 0.769 mday^{-1} and 40.47 to 8292.0 day^{-1} respectively. This research revealed high hydraulic conductivity in the western part implying good groundwater potential with moderate to high protective capacity while areas with low hydraulic conductivity correspond to areas with high resistivity indicating little or no pore space and total devoid of water. The hydraulic resistance quantifies groundwater vulnerability using AVI and reveals that the area of study is characterized by low to high AVI with moderate AVI dominanting. **Originality and novelty:** The estimated geohydraulic properties from resistivity data and their spatial spread are promising and could increase the depth of knowledge on groundwater vulnerability within and around the study area.

Keywords: VES; ERT; AVI; hydraulic conductivity; hydraulic resistance

1 Introduction

Socio-economic development depends majorly on water considering its importance on plants, animals and human activities such as agricultural industry, manufacturing industry, transportation industry, construction industry, home usage and life which cannot be overemphasized[1],[2]. The abundance and value of groundwater resources transcends from generation to generation. Health awareness through science and technology increased the quest for water that is fresh and free from contamination since our surface water (rivers, seas, oceans, ponds, lakes, springs and streams) are believed to be easily polluted[3]. Hence the need for adequate, clean, safe and good quality water source in both rural and urban areas becomes necessary. Groundwater quality is generally considered to be superior to surface water[4] because of the purifying effects of the soil column as a result of the earth acting as natural sieve during the process of percolation.

Sedimentary rocks have larger thickness[5], aquifer in sedimentary basin might lie in the deeper layers, considering the depths to the aquifer layer may scare individuals from drilling in this area without actually getting geophysical information. In some cases residents drilling to get potable groundwater face challenges of boreholes not yielding to satisfaction, not being able to get to the water table, contamination of the extracted groundwater in taste or odor. In addition, Nigeria is listed as one of the countries among 39 countries in the SubSahara Africa that practice open defecation[6] making ground water an unsafe source of drinking water for many areas[7]. The potential for ground water to become contaminated through human activities on the earth surface has come to lime light in recent years. Once contaminated, it is very difficult and costly to clean up ground water while in many attempted cases, it becomes impossible to achieve within a reasonable time[8],[9]. There is a relatively high cost of replacing unsafe sources with bottle treated water or other measures than existing potable ground water resources[10].

The contamination of the aquifer depends on factors like the depth to the aquifer, concentration of contaminants, and permeability of subsurface layers, geological setting and the direction of groundwater flow[11–13]. In determining the quality of groundwater, the geochemical or biogeochemical mineral composition of aquifer rocks and groundwater flow are considered. The flow of these minerals helps in determining the direction of contaminant flow in the groundwater. Although the mineralized water has agricultural benefits, environmental and human health conditions can be negatively affected.

The chemicals in the waste are dissolved by water (a process called leaching) resulting in contaminants, which has the potential to pollute groundwater resources. The electrical properties of the groundwater change as a result of the contaminants percolating into the subsurface[14]. There is need for proper knowledge of the subsurface geology since uncontaminated groundwater will serve as a major source of water supply. Wildcat drilling has exposed many groundwater repositories to contamination due to inadequate geologic knowledge of the location of water-bearing sediments[4],[15],[16] because lack of knowledge about location of aquifer in the study area and illegal drilling without getting to the aquifer made groundwater repositories in the area prone to contamination. Electrical resistivity methods enable the detection of contamination plumes due to the large contrast in the electrical conductivity of contaminated fluids relative to that of groundwater[17]. The integration of geophysical and physicochemical methods in assessing groundwater quality gives precise and valuable results, since the physicochemical method helps in confirming the behavior of groundwater to resistivity measurements[18]. Generally, the electrical resistivity method is preferred in a groundwater study due to its high resolving power, economic viability and it's minimal to non-invasiveness. In a geophysical survey, the measured physical parameters are unique, as these parameters give anomalous signatures of which the interpretation is important.

Researchers have employed the electrical resistivity method in characterizing groundwater problems related to aquifer potentiality to yield water[4],[16],[19–24] and contamination by delineating vulnerable zones, migration and the extent of contamination[11],[4,25–34]. AVI has also been employed to quantify the aquifer vulnerability of an area and has been proven to be simple, faster and is widely used by researchers[35–37]. The use of electrical resistivity method is very important in environmental monitoring and assessment. This method is centered on the reaction of the earth subsurface to the passage of current and the vertical electrical sounding (VES) employed to measure the vertical variations of resistivity with depth.

The conductivity of most contaminants are much higher than the conductivity of natural groundwater, and this large gap in conductivity values enables contamination plumes to be easily indentified using geophysical methods. The electrical resistivity methods (VES and ERT) are very useful in studying groundwater contamination due to the conductive state of most contaminants[17]. The use of VES and ERT gives a detailed knowledge of the features of aquifer hydrogeological units and detection of the contaminant plume. 2-D resistivity imaging (ERT) also has the probing power to reveal the vertical and lateral variation in resistivity related to changes in water content, chemical content and contaminant flow rate[38]. Also through the identification of fractured and weathered zones, the chance of drilling successfully has been improved[39]. The objectives of this study are to employ integrated electrical resistivity methods to assess susceptibility of groundwater to surface contamination, delineate the potential site for groundwater development and identify the possible vulnerable zones.

1.1 Location and Geology of the Study Area

The study area falls within the Anambra sedimentary Basin of the lower Benue Trough in the northern part of Enugu state comprising Nsukka, Igbo-Eze north, south and Udenu local government area of Enugu state. The coordinates of the study area lies between latitudes 6°80'N-7°03'N and longitudes 7°15'E – 7 °31'E (Figure 1). It covers a total surface area of approximately 3961 km^2. The main geomorphic features comprise high peaked hills and undulating slopes criss-crossed with dry valleys. The vegetation is guinea-savanna type. The topography is highly undulating with elevation which varies between 281 and 521 m above sea level measured in the field and is peaked at Umuabo-Ehalumona area at 521 m (Figure 2). There is a gentle downward slope E-W direction because of the fragile nature of the sandstone. The western part of the study area has numerous gully sites and valleys while the eastern portion is dominated by the cuesta topography.

The three main outcrop formations in the area are the Nsukka Formation (Upper Maastritchian) that presents essentially as outliers and laterite crusts in the hilly areas, the Ajalli Sandstone (Middle Maastritchian) made up of friable cross bedded sandstone that is the main aquifer and the underlying Mamu Formation (Lower Maastritchian) which comprises sandstone, shales, sandy-shales and coal outcrops towards the eastern extremity of the Nsukka area. Eroded remnants of the Nsukka formation forms outliers with a thickness average of 250 m [40] and springs which produces perched aquifer systems found within topographically controlled flow cells that are not in hydraulic continuity with adjacent cells which dry up during dry seasons [41–45]. The variation of the depth to perched water table varies between 3–10 m below the surface throughout the area and is solely affected by season and relative elevation.

The Nsukka and Ajalli formations belong to the same hydrostratigraphic unit [45], with thick water table aquifers. Since the hydraulic setting of Nsukka formation does not allow spring formation, water flows vertically downward to contribute to the regional system produced mainly by the Ajalli Sandstone. Regional flow is essentially from east to west. However, the Ajali sandstone harbors most of the aquifer layers with aquitard units [46] and consist of medium to coarse sand that forms the aquifer while the thin clays, silty clays and fine-grained sand units of the formation form the aquitards. Aquitards in the area are not evidently formed at the upper horizons. The 5.07 runoff percentage is insignificant when compared to the high permeability of the underlying soil mantle and Ajali sandstone that directly lies under the soil across the area [44].

The aquifer table water in this area lies in the middle to upper layers of Ajali sandstone and in the upper layers of the Manu formation constituting zones that partially recharges the deeper-seated confined aquifers [47],[48]. The northwestern part of the area are mostly lowlands serving as reservoir collecting almost all the run offs during the rainy season. The two seasons are the dry season and the rain season. The dry season is completely devoid of moisture and starts from November to April. Temperatures attain maxima of 34 degrees in the dry season and can attain minima of 22 degrees during the rainy season. Precipitation is high and approximate 1650mm/yr.

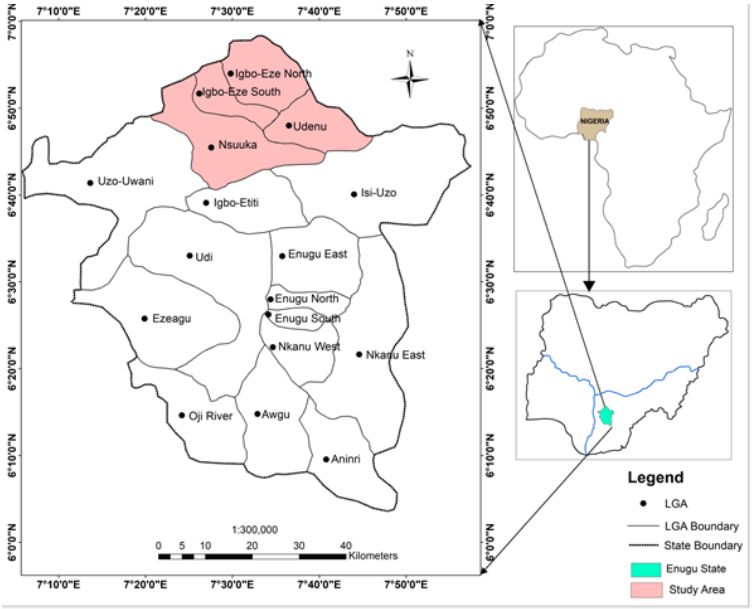

Fig 1. Location map of the study area

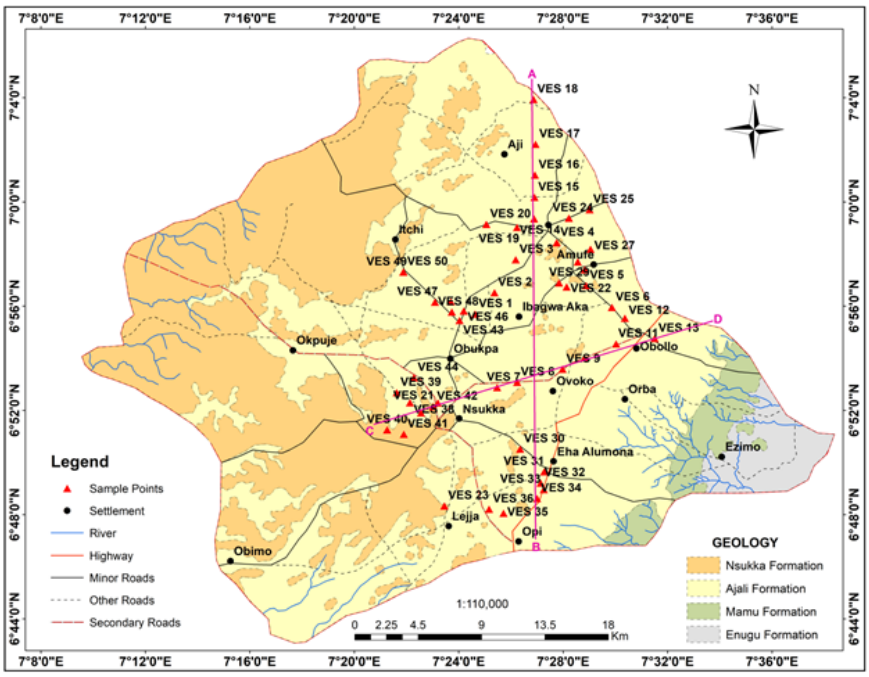

Fig 2. Geologic map of the study area

2 Methodology

An IGIS resistivity meter was used to carry out electrical resistivity survey on the ground surface to measure the resistivity distribution of the subsurface. The current and potential electrodes served as the transmitting and receiving cables to take resistivity readings of fifty vertical electrical soundings carried out within the study area using Schlumberger electrode configuration. This was done with half current electrode spacing (AB/2) ranging from 1.0 to 450.0 m and half potential electrode spacing (MN/2) of 0.25 to 40.0 m. Maximum current electrode spacing (AB) was maintained from one location to another considering areas of high and low elevation and settlement pattern in terms of good accessible paths for cables to be extended up to 900.0 m to ensure deeper depths. The computation of the apparent resistivity (ρ_a) was done using the values of the apparent resistance (R_a) and geometric factor (G_S) for Schlumberger array.

$$\rho_a = K\frac{v}{I} = G_S.R_a \tag{1}$$

Where G_S is the geometric factor for Schlumberger array mainly affected by electrode arrangement and R_a is the field apparent resistance measured from the equipment. Equation (1) can also be written as

$$\rho_a = \pi.\left[\frac{\left(\frac{AB}{2}\right)^2 - \left(\frac{MN}{2}\right)^2}{MN}\right].R_a \tag{2}$$

where AB is the distance separating the two current electrodes while MN is the separating distance between the potential electrodes, and where

$$G_S = \pi.\left[\frac{\left(\frac{AB}{2}\right)^2 - \left(\frac{MN}{2}\right)^2}{MN}\right] \tag{3}$$

The field sounding point coordinates were measured using global positioning system instrument. The obtained apparent resistivity values were plotted on a bi-logarithm graph at half electrode spacing and the smoothening of the curves was done by

employing the linear vertical scales to suppress the effects of lateral inhomogeneities and near surface layers viewed as noise. The pattern of variation of resistivity gives information on the subsurface layers, structures of formations that eventually give rise to some sounding curves.

The least square inversion of filtered resistivity curve to true resistivity was electronically carried out using a flexible WINRESIST software program. The electronic analysis produced VES curves with reasonable acceptable fit and gives the primary geoelectric true resistivity, thickness and depth after series of repetitions with minimal RMS acceptable error margin. Figures 3, 4 and 5 is typical geoelectric curves obtained from the computer aided analysis whose depths were constrained using borehole logs as shown in Figure 6. The depth values were constrained because of the intrinsic problems of equivalence and suppression that affect and make it difficult to quantitatively interpret VES data. It also helps to reduce the choice of layer models through adjusting the layer thickness and depths as the resistivity varies at point of contamination [49], [50].

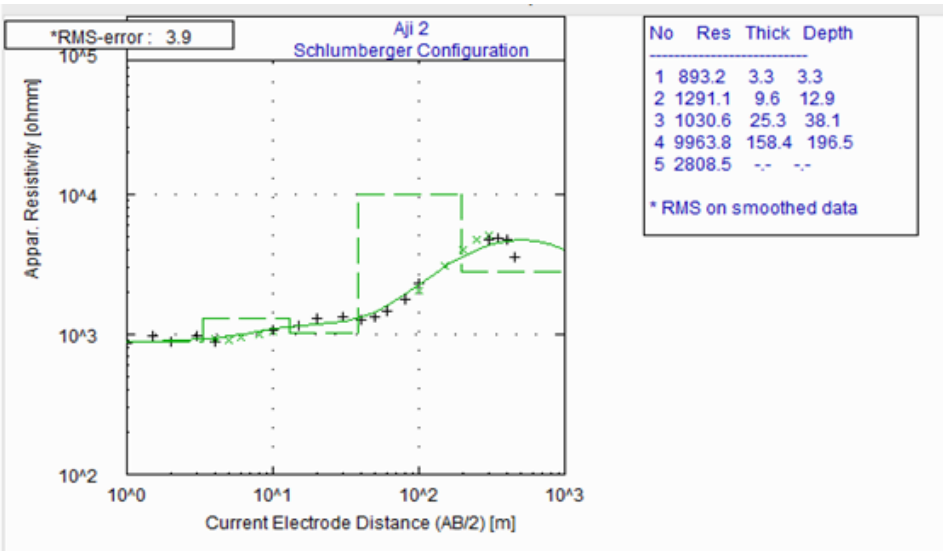

Fig 3. Geoelectric curve for VES14

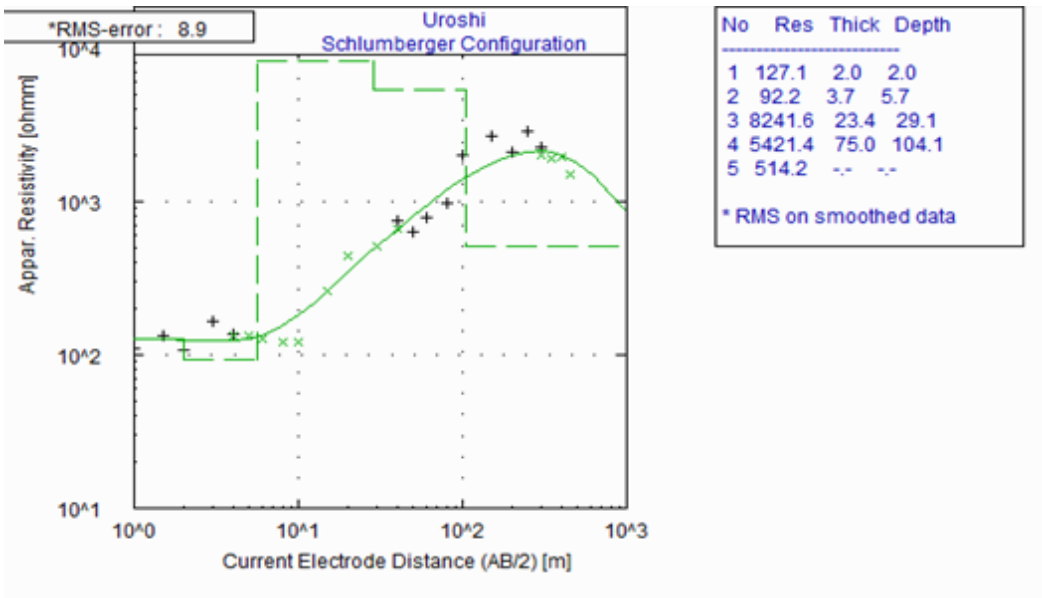

Fig 4. Geoelectric curve for VES26

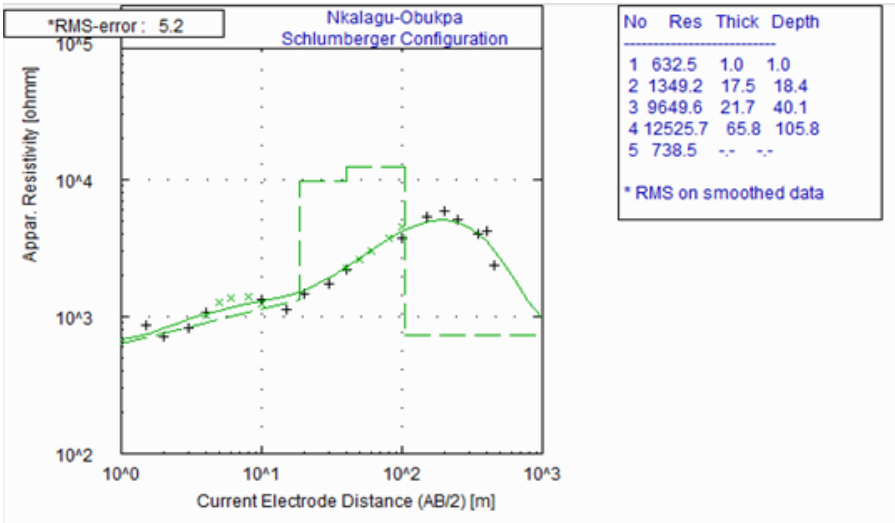

Fig 5. Geoelectric curve for VES50

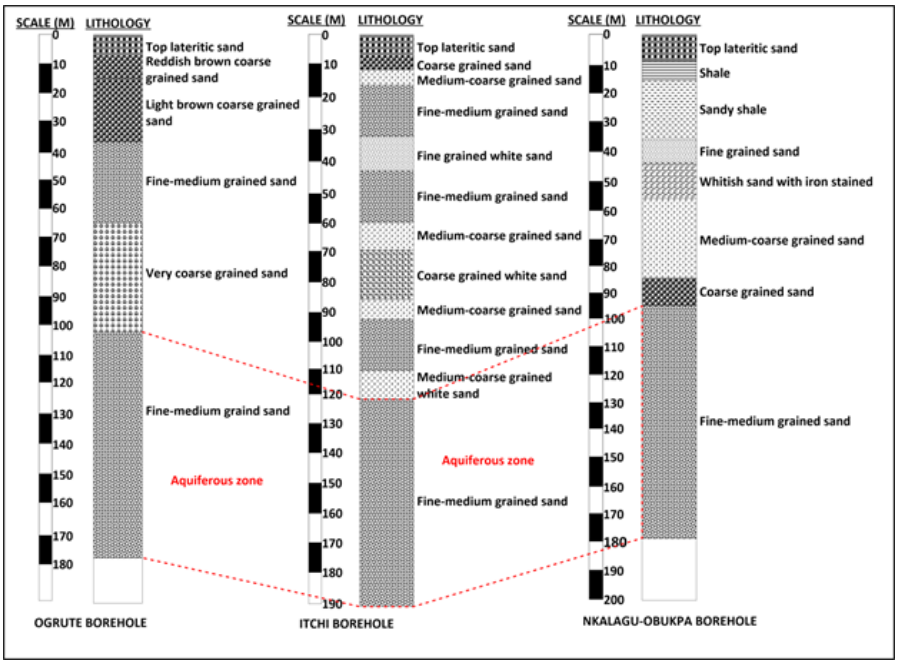

Fig 6. Borehole lithology logs. a: borehole lithologic log close to VES 17, b: borehole lithologic log closeto VES 26 c: borehole lithologic log close to VES 50

The two fundamental parameters layer resistivity (ρ) and depth (h) describe a geologic unit and are necessary in the interpretation of electrically stratified earth models. These quantities are essential in calculating the hydraulic conductivity and hydraulic resistance for homogenous horizontal layers[35],[51]. The porous and fractured nature of the subsurface rocks is an indication that groundwater moves easily through the pore spaces and this describes hydraulic conductivity better. The vulnerability of the aquifer protective layers is assessed using the hydraulic conductivity which according[52], can be computed using in Equation (4).

$$K = 386.40\rho^{-0.93282} \tag{4}$$

where K is the hydraulic conductivity and ρ is the aquifer resistivity.

According to [35], there is an easy and quick estimation method known as aquifer vulnerability index (AVI) that uses the vertical hydraulic conductivity K and the thickness h of the layers overlying the water table to calculate the hydraulic resistance. This index evaluates the aquifer vulnerability through the estimated hydraulic resistance of each layer to vertical flow of water and expresses the estimated value of the average travel time of a contaminant from the surface to the subsurface water table [53]. (Table 1) was used in rating the vulnerability of aquifer layers after the computation of hydraulic resistance. The hydraulic resistance (C) was computed using the two parameters and is expressed as:

$$C = \sum_{i=1}^{n} \frac{h_i}{K_i} \tag{5}$$

where h_i is thickness and K_i is hydraulic conductivity of each covering layer.

Table 1. Relationship between aquifer vulnerability index (AVI) and hydraulic resistance [35]

Hydraulic resistance (C)	log C	Vulnerability (AVI)
0–10	< 1	Extremely high
10–100	1–2	High
100–1000	2–3	Moderate
1000–10,000	3–4	Low
> 10,000	> 4	Extremely low

The study area was also surveyed using the IGIS resistivity meter employing the Wenner electrode configuration which yielded a detailed five ERT profiles by allowing equal electrode spacing (a) of 5 m between the pairs of current and potential electrodes throughout the entire survey. All electrodes were moved at interval of 5 m, 10 m, 15 m, 20 m, to 65 m until the half separation 200 m and maximum length of 400 m was exhausted. The Wenner electrode configuration is very prone to variations in the subsurface resistivity which occurs in the vertical direction and can solve problems resulting from vertical changes in the subsurface [54]. Also Wenner electrode array have the ability to produce set of data with high signal to noise ratio [55]. Equation 6 was used to calculate the apparent resistivity values for the 2D imaging from the measured field resistance values which was further processed using RES2DINV×32 version 3.71.115 software package.

$$\rho_{a=2\pi} \frac{\triangle v}{I} a \tag{6}$$

The geometric factor G_W for Wenner is given by:

$$G_W = 2\pi a$$

where a is the electrode separation.

3 Results and Discussion

The quantitative interpretation of the VES data gave resistivities, thicknesses and depths values within the maximum current electrode separation and also revealed five to six geoelectric layers and is shown in (Supplementary table 2). Layer one has resistivity ranging from 40.4 to 3367.1 Ωm with depth and thickness value within the range of 0.5 to 3.9 m which can be delineated as lateritic sand at the surface. The resistivity range of the second layer is between 92.2 to 11730.1 Ωm with corresponding thickness and depth ranging from 1.5 to 20.4 m and 2.6 to 23.2 m respectively. The lithology third layer can be described as coarse sand with varying resistivity values ranging from 85.3 to 73324.3 Ωm while its thickness and depth values ranges from 3.6 to 85.7 and 8.9 to 94.6 m. The fourth layer is associated with relatively high values of resistivity from 153.7 to 91659.2 Ωm with its respective high thickness and depth values ranging from 22.4 to 174.3 m and 31.3 to 218.4 m. This shows that it is extremely resistive when compared with the resistivity of the overlying layers, this lithologic unit harbors about 84% of the aquifer in the area. The fifth layer has resistivity range of 312.8 to 16675.1 Ωm with undefined thickness and depth values except for VES 3, 8, 12, 13, 24, 23 and 38 with range of 45.1 to 154.4 m and 104.3 to 198.0 m. This layer is less resistive and more conductive than the overlying layers harboring 14% of the aquifers within the area. The sixth layer is observed only in VES 3, 8, 12, 13, 24, 23 and 38 with resistivity range of 1118.9 to 6892.0 Ωm and a totally undefined thickness and depth values in all the VES stations. Since this layer is below the water table, the sediments in this lithologic unit are considered to be unconsolidated [56]. (Figures 7 and 8) shows the variation of resistivities with depths in the geoelectric section along transect AB

and CD (Figure 2) which cuts across VES 18, 17, 16, 15, 14, and 36 and VES 38, 42, 7, 8, 9, 13 respectively. The earth materials that dominates the subsurface are fine-medium grain sand, coarse grain sand, dark grey shale, fine grain sand, medium-coarse grain sand, the fine grain sand and the coarse grain sand harbors most of the aquifer layers. The values of resistivity in Ohm-m at various depths are indicated within the location and resistivity range that is geologically equivalent within the penetrated depth is also shown.

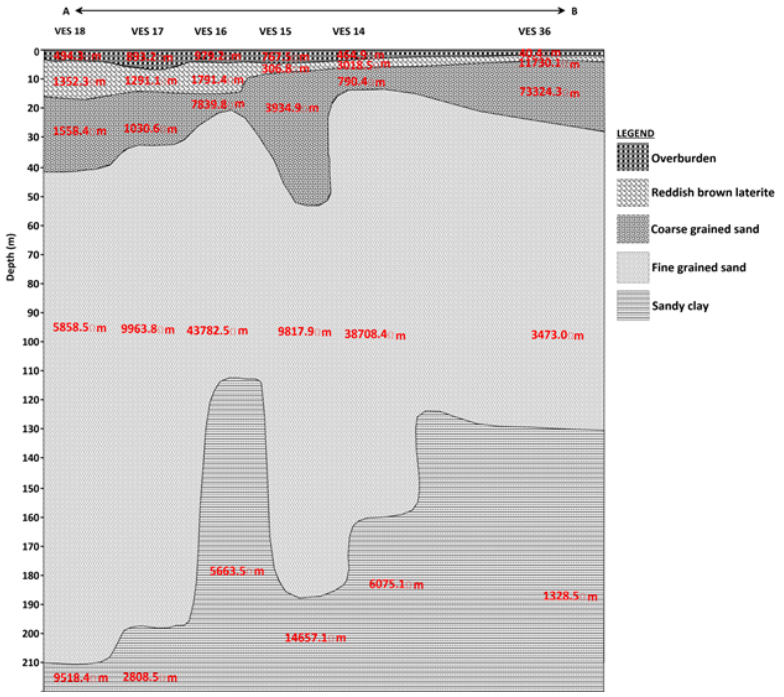

Fig 7. Geoelectric section across transect AB

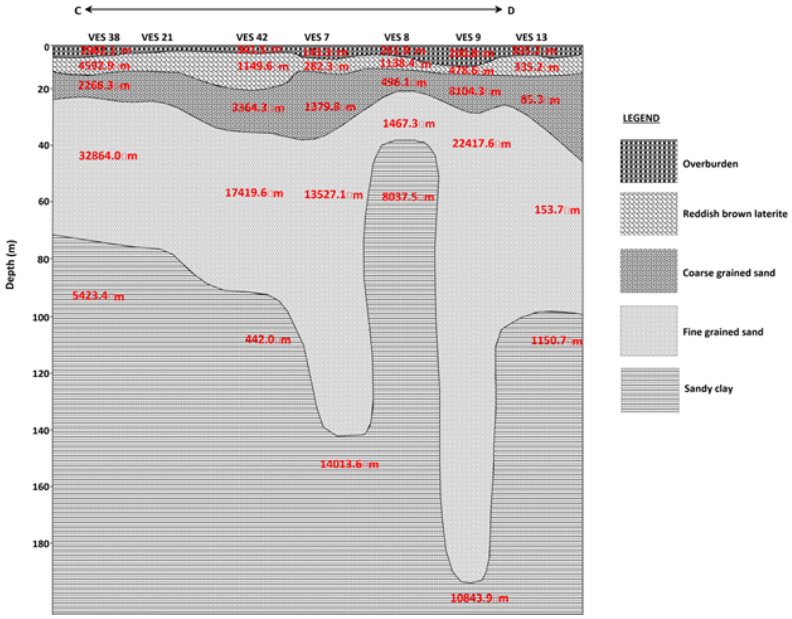

Fig 8. Geoelectric section across transect CD

Overburden resistivity ranged from 589.8 to 85094.8 Ωm having an average value of 42642.3 Ωm with high values at the southwestern part while low values spreads across other parts of the area (Figure 9). Thickness range of 8.9 to 99.5 m having an average value of 54.2 m was high at the northeastern and southwestern part while other parts have low thickness (Figure 10). This shows that some locations in the northeastern and southwestern part of the area is delineated as zones with the highest overburden thickness indicating areas with high protective capacity. The compact nature of the geomaterials at the top layers is as a result of high resistivity values of the constituents. From the result, it is noted that most areas with high thickness corresponds to areas of low resistivity.

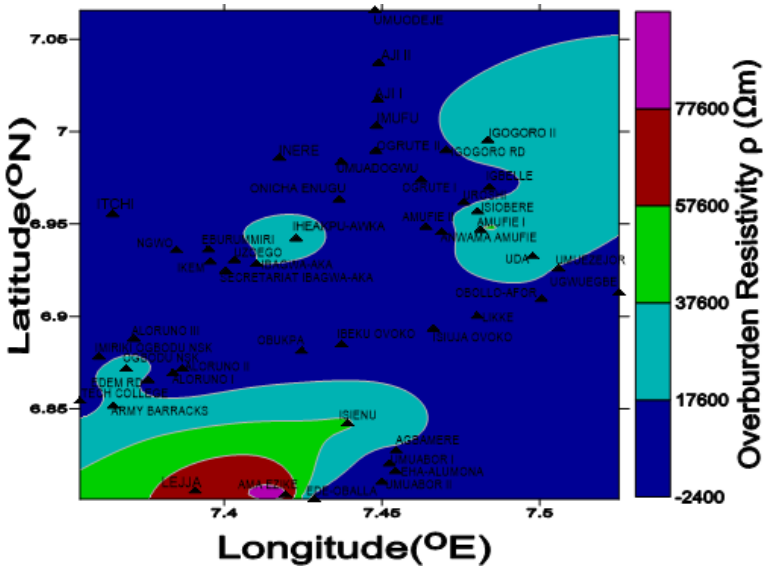

Fig 9. Contour map showing variation of overburden resistivity in the study area.

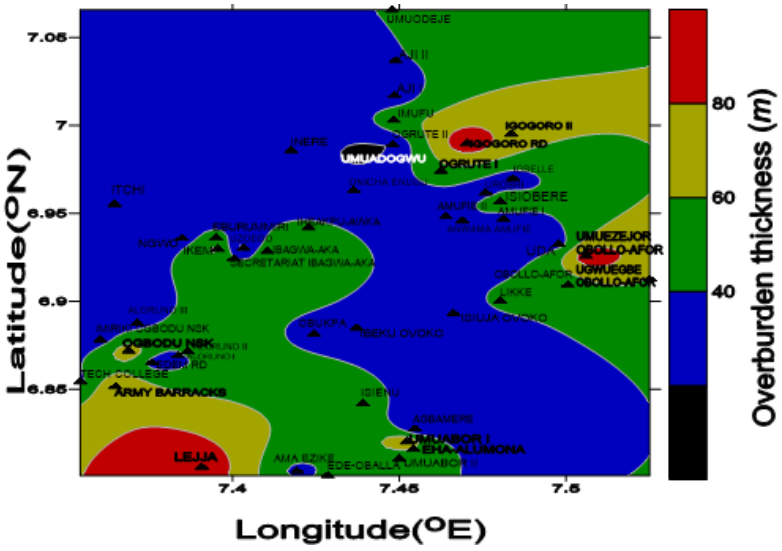

Fig 10. Contour map showing variation of overburden thickness in the study area.

The computed hydraulic conductivity (K) was contoured (Figure 11), and its variation ranges from 0.010 to 0.769 m day^{-1} indicating that the western part of the area has high values of hydraulic conductivity while low values spreads from the north down to contour map showing variation of overburden thickness in the study area. The southern parts of the study. The variation of hydraulic conductivity parameter indicates the existence of clay stone argillites below the surface and characterizes the changing behavior of an aquifer to allow groundwater to pass through the protective layers [37].

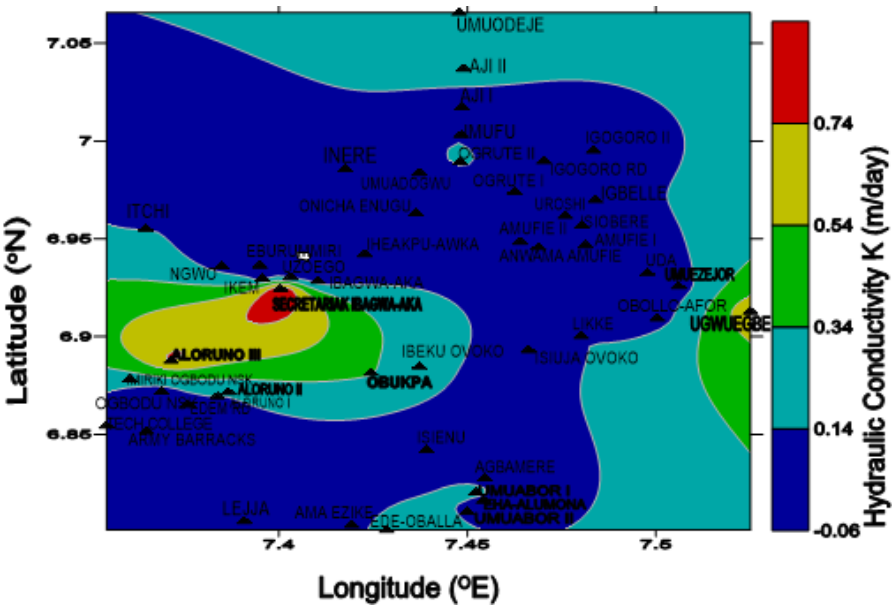

Fig 11. Contour map showing variation of hydraulic conductivity in the study area.

The hydraulic resistance is the key parameter in quantifying groundwater vulnerability which indicates the protective capacity of the aquifer layer. Its values range from 40.47 to 8292.0 secs. The capacity of geomaterials to delay the infiltration of fluid into the subsurface is an estimation of its protective capacity because geomaterial naturally sieve the percolating fluid[57], [58]. The relationship between the aquifer vulnerability index (AVI), C and log C is shown in (Table 1) while (Supplementary table 3) shows that in most of the locations (29 locations), the rating of AVI was moderate and VES 7, 13, 43 and 44 rated high according to[35]. (Figure 12) is a contour map showing the distribution of hydraulic resistance and the variation of the vulnerable zones across the area. It shows that part of southwest has moderate to high protective capacity while the zones with low protective capacity dominates the study area. The southwestern zone with high hydraulic resistance can be delineated as zone having low permeability which indicates high clay volume while zones with low values have high permeability and low clay content thus are vulnerable to contamination.

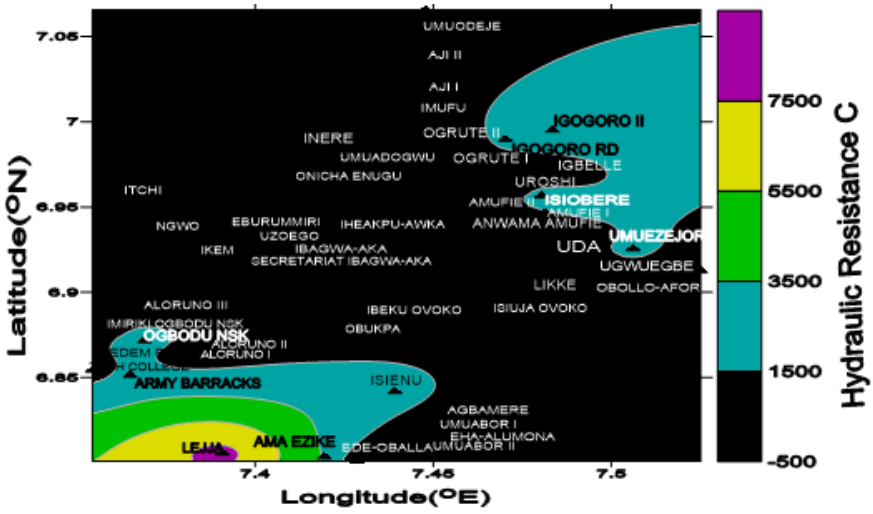

Fig 12. Contour map showing variation of hydraulic resistance in the study area.

Also, these zones with high resistive materials have high hydraulic resistance. The hydraulic resistance has an indirect relationship with hydraulic conductivity. The model results of five surveyed ERT profiles are shown in (Figures 13, 14, 15, 16 and 17). The inverted models clearly displayed variation in the subsurface resistivity, and delineated high and low resistivity zones. These five profiles were taken close to VES points 2, 1, 7, 47, and 24 respectively. In profile 1 (Figure 13), located at Iheakpu- Isiugwu near VES 2 the resistivity distribution zones of low to mean resistivity (blue color) of outcropping gnesis ranging from 0 to 549 Ohm m and a decreasing thickness from about 19.8 m at the beginning to 6.8 m toward the center and increases to 12.4 towards the east. At a depth of 9.8 m and lateral distances of 70 to 110 m and 170 to 187m appears a more conductive and lower resistivity layer indicating the presence of saturated sand with contaminated plumes. Below the topsoil unit appears a weathered layer with increased resistivity ranging from 550 to 12400 Ohm m with an increasing thickness from about 19.8m to 28.7 m and decreases toward the center. It is followed by a high resistivity with depth which represents weathered gneiss. Beyond 28.8 m depth, the high resistivity (reddish color) values ranging from 12400 to 34872 Ohm m indicates the presence of a massive gneiss rock, with no tectonic fracture in the sedimentary rock showing total devoid of water and insignificant hydrogeological prospecting. Hence, the aquifer layer is located at a shallow depth and can be exposed to contamination within a short time because its vertical travel time will be small.

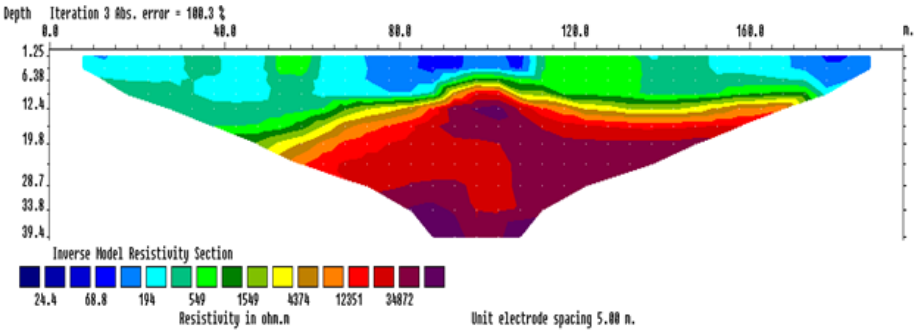

Fig 13. ERT profile 1 near VES 2

Profile 2 (Figure 14) is located at Ibagwa-aka I near the VES 1 showing three layer formation. The continuous top soil surface layer has mean resistivity (green-yellow color) ranging from 120 to 544 Ohm m located (west) within lateral distance from 20 to 80 m and a highly weathered gnesis with high resistivity value ranging from 550 to 1150 Ohm m. This top soil is composed of lateritic sandstone with thickness ranges from 1.3 to 13 m. Underlying the top soil is a highly resistive formation with resistivity ranging from 1150 to above 2430 Ohm m which appears at a depth between 13 and 33.8 m. This low conductive layer is covered under by a mean weathered conductive geomaterials associated with moderate infiltration and permeability of the layers. Hence, this mean resistive layer at the depth of this profile indicates presence of moderately conductive geomaterial which can be as a result of downward migration of contaminants to the groundwater over a long period of time through an early formation fracture between lateral positions of 65 to 90 m.

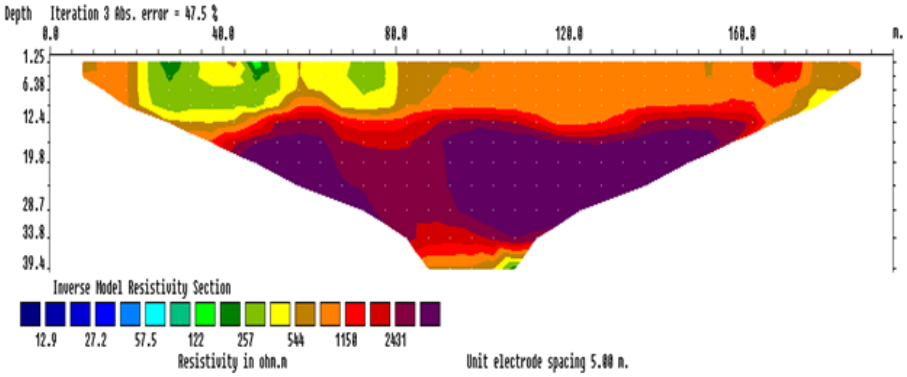

Fig 14. ERT profile 2 near VES 1

Profile 3 situated at Ibige Obukpa close to VES 7 (Figure 15), shows a thick layer of undulating resistive materials as the topsoil with moderate resistivity value ranging from 330 to 1400 Ohm m and approximated thickness ranging from 1.25 to 12.4 m. A freshly weathered laterite appears at the middle of the profile between lateral distances of 75 to 120 m. Below this unit appears a high resistivity lateritic formation showing smooth variations of resistivity which ranges from 1400 to 2910 Ohm m and above with an increasing thickness from 13 m down covering the entire profile. This layer has low conductivity and lacks enough conducting fluids, impermeable layers with low porosity. Thus, the topsoil is fairly protected from contamination.

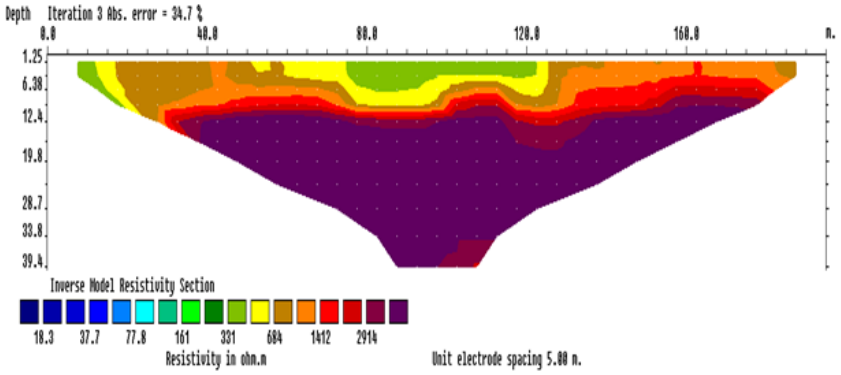

Fig 15. ERT profile 3 near VES 7

Profile 4 is the 2D inverted resistivity model at Ibagwa-aka II site near VES 47 (Figure 16), shows a prominent lateral heterogeneous layer of resistive materials as the topsoil with mean resistivity ranging from 130 to 400 Ohm m and a thickness from about 6.38 m at the beginning to 9.3 m toward the end which represents the outcropping gneiss. Below the topsoil at a depth of 9.3 to 20 m (NW) and 9.3 m (SE) deep down at a lateral distance of 15 to 80 m and 105 m to 175 m appears a layer with higher resistivity values ranging from 1230 to 11894 Ohm m. After this highly resistive unit lies a low resistive layer with values ranging from 4.26 to 128 Ohm m at a depth of 20 m down located (SW) at lateral distance of 55 to 95 m. This low resistivity zones surrounded by high resistivity and impermeable rooftops suggests a captive aquifer zone may have the possibility of being contaminated from an unconfined layer or through fracture or slow movement of fluids through the highly resistive surrounding layers over time.

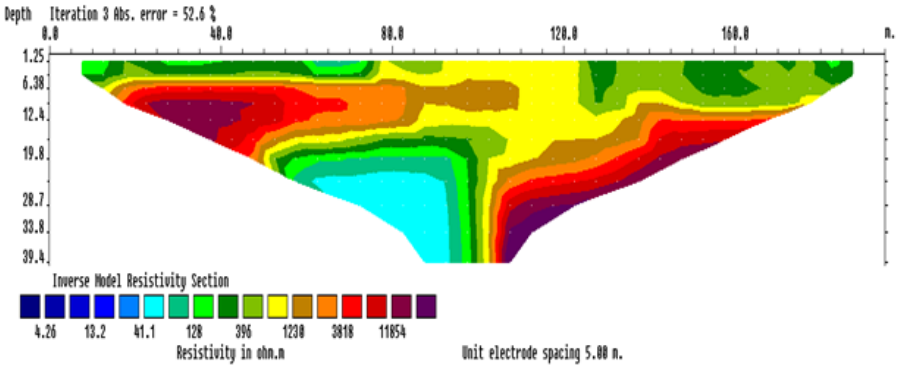

Fig 16. ERT profile 4 near VES 47

The fifth profile (Figure 17) is located at Nkpamute Igogoro near VES 24. The topsoil and the deeper layers has low resistivity while the middle of the profile has high resistivity value from a depth of 6 m down to 25 m and spreads across the profile from west to east. The low resistivity at the topsoil indicates the presence of high conductive materials that moves gradually seeping down to the aquifer layer. There is a highly resistive second layer formation which could be associated with the lateritic formation present in the area showing smooth variations of resistivity which ranges from 977 to 8938 Ohm m located between lateral distance of 40.0 to 180.0 m with an increasing thickness from 6.34 m to 24 m and increased to33.8 m toward the southeastern part of the section. The third layer formation appears conducting with very low resistivity ranging from 3.86 to 35.3 Ohm m. This

layer is relocated between electrodes positions 80 to 110 m at a depth of 35 m down indicating a potential groundwater target. This very low resistivity zone that is confined by high resistivity and impermeable rooftops suggests a captive uncontaminated aquifer zone.

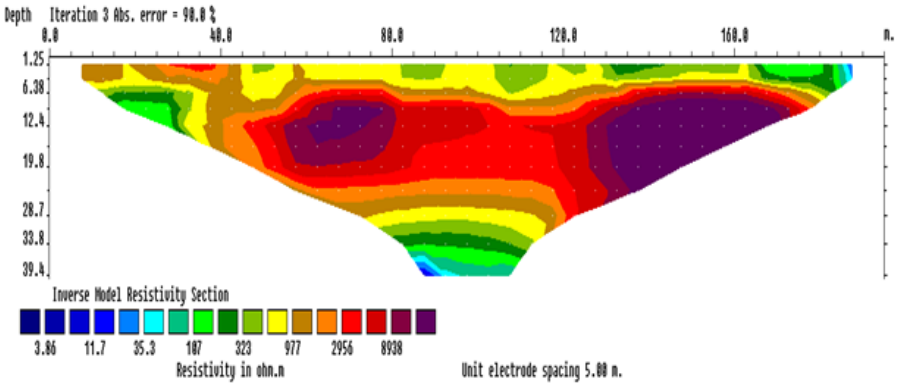

Fig 17. ERT profile 5 near VES 24

4 Conclusion

The hydrogeologic unit of the area was assessed using the results from VES and ERT profiles. The aquifer layer in the area lies between the fourth and fifth geoelectric layers, the fourth layer harbors up to 84% of the aquifers at thickness and depth values ranging from 22.4 to 174.3 m and 31.3 to 218.4 m. The values of aquifer geoelectric parameters vary across the subsurface. The estimated aquifer vulnerability index (AVI) of the protective layers helps in evaluating the vulnerability of the study area and delineation of vulnerable zones within the study area. The contour maps displayed the distribution of these parameters, revealing the changes in the subsurface in homogeneity. High hydraulic conductivity was observed at the southwestern part of the area implying that the region is good for groundwater potential as a result of low elevation and direction of runoff water during the wet season. VES locations having high vulnerability index indicates that the aquifers within these locations will be highly vulnerable to surface contaminants. The ERT profiles show the distribution of subsurface resistivity with depth. The results from this study have rated the vulnerability status of the hydrogeologic units and also give information that will be important in groundwater exploration and management.

References

1) Igor AS. World water resources: A new appraisal and assessment for the 21st century. International hydrological progrramme. 1998.
2) Obiora DN, Ibuot JC, Alhassan UD, Okeke FN. Study of aquifer characteristics in northern Paiko, Niger State, Nigeria, using geoelectric resistivity method. *International Journal of Environmental Science and Technology*. 2018;15(11):2423–2432. Available from: https://dx.doi.org/10.1007/s13762-017-1612-8.
3) Edet A, Worden HR. Monitoring of the physical parameters and evaluation of the chemical composition of river and groundwater in Calabar (Southeastern Nigeria). *Environmental Monitoring and Assessment*. 2009;157(1-4):243–258. Available from: https://dx.doi.org/10.1007/s10661-008-0532-y.
4) George NJ, Nathaniel EU, Etuk SE. Assessment of Economically Accessible Groundwater Reserve and Its Protective Capacity in Eastern Obolo Local Government Area of Akwa Ibom State, Nigeria, Using Electrical Resistivity Method. *ISRN Geophysics*. 2014;2014(3):1–10. Available from: https://dx.doi.org/10.1155/2014/578981.
5) Chapman RE. Petroleum geology. Amsterdam. Elsevier. 1983.
6) UNICEF and WHO. Progress on drinking water, sanitation and hygiene: 2000-2017. Joint monitoring program for water supply (JMP). Newyork, Geneva. 2019.
7) National Water Summary 1987: Hydrologic Events and Water Supply and Use. U. S. Government Printing Office. Washington D.C. 1990.
8) Mackay MD, Cherry AJ. Groundwater contamination: pump-and-treat remediation. *Environmental Science & Technology*. 1989;23(6):630–636. Available from: https://dx.doi.org/10.1021/es00064a001.
9) Haley LJ, Hanson B, Enfield C, Glass J. Evaluating the Effectiveness of Ground Water Extraction Systems. *Groundwater Monitoring & Remediation*. 1991;11(1):119–124. Available from: https://dx.doi.org/10.1111/j.1745-6592.1991.tb00358.x.
10) Abdalla CW. Measuring economic losses from ground water contamination: An investigation of household avoidance costs. *Journal of the American Water Resources Association*. 1990;26(3):451–463. Available from: https://dx.doi.org/10.1111/j.1752-1688.1990.tb01384.x.
11) Lopes DD, Silva MCPS, Fernandes F, Teixeira SR, Celligoi A, Dall'Antônia LH. Geophysical technique and groundwater monitoring to detect leachate contamination in the surrounding area of a landfill – Londrina (PR – Brazil). *Journal of Environmental Management*. 2012;113:481–487. Available from: https://dx.doi.org/10.1016/j.jenvman.2012.05.028.
12) Bayode S, Adeniyi KE. Integrated geophysical and hydrochemical investigation of pollution associated with the IIara Mokin dumpsite. *American International Journal of Contemporary Research*. 2014;4(2):150–160. Available from: www.aijcrnet.com.

13) Ibuot CJ, Obiora ND, Ekpa MMM, Okoroh OD. Geoelectrohydraulic investigation of the surficial aquifer units and corrosivity in parts of Uyo L. G. A., Akwa Ibom State, Southern Nigeria. *Applied Water Science*. 2017;7(8):4705–4713. Available from: https://dx.doi.org/10.1007/s13201-017-0632-3.
14) Al-Tarazi E, Rajab JA, Al-Naqa A, El-Waheidi M. Detecting leachate plumes and groundwater pollution at Ruseifa municipal landfill utilizing VLF-EM method. *Journal of Applied Geophysics*. 2008;65(3-4):121–131. Available from: https://dx.doi.org/10.1016/j.jappgeo.2008.06.005.
15) Ibuot JC, Akpabio GT, George NJ. A survey of the repositories of groundwater potential and distribution using geoelectrical resistivity method in Itu Local Government Area (LGA). *Central European Journal of Geosciences*. 2013;5(4):538–547. Available from: https://doi.org/10.2478/s13533-012-0152-5.
16) Ibanga IJ, George JN. Estimating geohydraulic parameters, protective strength, and corrosivity of hydrogeological units: a case study of ALSCON, Ikot Abasi, southern Nigeria. *Arabian Journal of Geosciences*. 2016;9(5):1–16. Available from: https://dx.doi.org/10.1007/s12517-016-2390-1.
17) Pomposiello C, Dapena C, Favetto A, Boujon P. Application of geophysical methods to waste disposal studies, municipal and industrial waste disposal. In: Yu Y, editor. Municipal and Industrial Waste Disposal. Rijeka, Croatia. InTech. 2012;p. 3–27. Available from: https://doi.org/10.5772/29615.
18) Abbaspour KC, Rouholahnejad E, Vaghefi S, Srinivasan R, Yang H, Kløve B. A continental-scale hydrology and water quality model for Europe: Calibration and uncertainty of a high-resolution large-scale SWAT model. *Journal of Hydrology*. 2015;524:733–752. Available from: https://dx.doi.org/10.1016/j.jhydrol.2015.03.027.
19) Bahar MM, Reza MS. Hydrochemical characteristics and quality assessment of shallow groundwater in a coastal area of Southwest Bangladesh. *Environmental Earth Sciences*. 2010;61(5):1065–1073. Available from: https://dx.doi.org/10.1007/s12665-009-0427-4.
20) Jimmy NG, Otu AA, Asuquo AU. Preliminary Geophysical Investigation to Delineate the Groundwater Conductive Zones in the Coastal Region of Akwa Ibom State, Southern Nigeria, around the Gulf of Guinea. *International Journal of Geosciences*. 2013;04(01):108–115. Available from: https://dx.doi.org/10.4236/ijg.2013.41011.
21) Akpan AE, Ugbaja AN, George NJ. Integrated geophysical, geochemical and hydrogeological investigation of shallow groundwater resources in parts of the Ikom-Mamfe Embayment and the adjoining areas in Cross River State, Nigeria. *Environmental Earth Sciences*. 2013;70(73):1435–1456. Available from: https://dx.doi.org/10.1007/s12665-013-2232-3.
22) George NJ, Ibuot JC, Obiora DN. Geoelectrohydraulic parameters of shallow sandy aquifer in Itu, Akwa Ibom State (Nigeria) using geoelectric and hydrogeological measurements. *Journal of African Earth Sciences*. 2015;110:52–63. Available from: https://dx.doi.org/10.1016/j.jafrearsci.2015.06.006.
23) Ibuot JC, Okeke FN, George NJ, Obiora DN. Geophysical and physicochemical characterization of organic waste contamination of hydrolithofacies in the coastal dumpsite of Akwa Ibom State, southern Nigeria. *Water Supply*. 2017;17:1626–1637. Available from: https://dx.doi.org/10.2166/ws.2017.066.
24) Ibuot JC, George NJ, Okwesili AN, Obiora DN. Investigation of litho-textural characteristics of aquifer in Nkanu West Local Government Area of Enugu state, southeastern Nigeria. *Journal of African Earth Sciences*. 2019;153:197–207. Available from: https://dx.doi.org/10.1016/j.jafrearsci.2019.03.004.
25) Mor S, Ravindra K, Dahiya RP, Chandra A. Leachate Characterization and Assessment of Groundwater Pollution Near Municipal Solid Waste Landfill Site. *Environmental Monitoring and Assessment*. 2006;118(1-3):435–456. Available from: https://dx.doi.org/10.1007/s10661-006-1505-7.
26) Abdullahi NK, Osazuwa IB, Sule PO. Application of integrated geophysical techniques in the investigation of groundwater contamination: a case study of municipal solid waste leachate. *Ozean Journal of Applied Sciences*. 2011;4(1):7–25. Available from: https://www.researchgate.net/328343633.
27) Ayolabi EA, Folorunso AF, Kayode OT. Integrated Geophysical and Geochemical Methods for Environmental Assessment of Municipal Dumpsite System. *International Journal of Geosciences*. 2013;04(05):850–862. Available from: https://dx.doi.org/10.4236/ijg.2013.45079.
28) Iyoha A, Akhirevbulu OE, Amadasun CVO, Evboumwan IA. 2D resistivity imaging investigation of solid waste landfill sites in Ikhueniro Municipality, Ikpoba Okha Local Government Area. *Journal of Resources Development and Management*. 2013;1:65–69. Available from: https://scholar.google.com/scholar/138147470716505071.
29) Syukri M, Saad R, Abubakar M. Leachate migration delineation using 2-D electrical resistivity imaging (2-DERI) at Gampong Jawa. *Banda Aceh Electronic Journal of Geotechnology England*. 2013;18:1505–1510. Available from: https://scholar.google.com/scholar/4411924849287169091.
30) Omolayo D, Tope FJ. 2D Electrical Imaging Surveys for Leachate Plume Migration at an Old Dump Site in Ibadan South Western Nigeria: A Case Study. *International Journal of Geophysics*. 2014;2014(2):1–6. Available from: https://dx.doi.org/10.1155/2014/879530.
31) Bayowa GO, Falebita DE, Adegboyega RO. Surface DC resistivity survey of contamination beneath Ido-Osun dumpsite. *Southern Nigeria Geofisca Internacional*. 2015;54(4):343–352. Available from: https://dialnet.unirioja.es.
32) Ganiyu SA, Badmus BS, Oladunjoye MA, Aizebeokhai AP, Olurin OT. Delineation of leachate plume migration using electrical resistivity imaging on Lapite dumpsite in Ibadan. *Southern Nigeria Geosciences*. 2015;5(2):70–80. Available from: https://doi.org/10.5923/j.geo.20150502.03.
33) Obiora DN, Ajala AE, Ibuot JC. Evaluation of aquifer protective capacity of overburden unit and soil corrosivity in Makurdi, Benue state, Nigeria, using electrical resistivity method. *Journal of Earth System Science*. 2015;124(1):125–135. Available from: https://dx.doi.org/10.1007/s12040-014-0522-0.
34) Ugwuanyi MC, Ibuot JC, Obiora DN. Hydrogeophysical study of aquifer characteristics in some parts of Nsukka and Igbo Eze south local government areas of Enugu State. *Nigeria International Journal Physical Science*. 2015;10(15):425–435. Available from: https://doi.org/10.5897/IJPS2015.4373.
35) Stempvoort DV, Ewert L, Wassenaar L. Aquifer vulnerability index: a GIS— compatible method for groundwater vulnerability mapping. *Canadian Water Resources Journal*. 1993;18(1):25–37. Available from: https://dx.doi.org/10.4296/cwrj1801025.
36) Putranto TT, Santi N, Widiarso DA, A D. Dimas Pamungkas D. Application of aquifer vulnerability index (AVI) method to assess groundwater vulnerability to contamination in Semarang urban area. MATEC web of conferences series. 2018. Available from: https://dx.doi.org/10.1015/matecconf/201815901036.
37) Obiora ND, Ibuot CJ. Geophysical assessment of aquifer vulnerability and management: a case study of University of Nigeria, Nsukka, Enugu State. *Applied Water Science*. 2020;10(1):1–11. Available from: https://dx.doi.org/10.1007/s13201-019-1113-7.
38) Ehirim CN, Ebeniro JO, Olanegan OP. A geophysical investigation of solid waste landfill using 2-D resistivity imaging and vertical electrical sounding methods in Port Harcourt municipality. *The Pacific Journal of Science and Technology*. 2009;10(2):604–613. Available from: https://www.akamaiuniversity.us/PJST.html.
39) Singh KKK, Singh KA, Singh KB, Sinha A. 2D resistivity imaging survey for siting water-supply tube wells in metamorphic terrains: A case study of CMRI campus, Dhanbad, India. *The Leading Edge*. 2006;25:1458–1460. Available from: https://dx.doi.org/10.1190/1.2405329.
40) Ezeh CC, Ugwu GZ. Geoelectrical sounding for estimating groundwater potential in Nsukka L.G.A. Enugu State, Nigeria. *International Journal of the Physical Sciences*. 2010;5(5):415–420. Available from: https://dx.doi.org/10.5897/IJPS.9000275.
41) Uma KO, Egboka BCE, Onuoha KM. New statistical grain-size method for evaluating the hydraulic conductivity of sandy aquifers. *Journal of Hydrology*. 1989;108(1-4):343–366. Available from: https://dx.doi.org/10.1016/0022-1694(89)90293-x.
42) Reyment RA. Stratigraphy of the Cretaceous and Cenozoic Deposits. In: and others, editor. Aspects of the Geology of Nigeria. Ibadan University Press. 1965.
43) Nwachukwu SO, Ofomata GEK. The Geology of Nsukka Area. The Nsukka Environment. *Nigeria*. 1978;p. 47–58.

44) Agagu OK, Fayose EA, Paters SW. Stratigraphy and sedimentation in the senonian Anambra basin of Eastern Nigeria. *Journal of Mining Geology*. 1985;22(1):25–36. Available from: https://bigf.ac.uk/africaGroundwaterAtlas/NG1101.
45) Egboka CEB, Uma OK. Comparative analysis of transmissivity and hydraulic conductivity values from the Ajali aquifer system of Nigeria. *Journal of Hydrology*. 1986;83(1-2):185–196. Available from: https://dx.doi.org/10.1016/0022-1694(86)90192-7.
46) Nwankwor GI, Egboka BC, Orajaka IP. Groundwater occurrence and flow pattern in the Enugu coal-mine area, Anambra State, Nigeria. *Hydrological Sciences Journal*. 1988;33(5):465–482. Available from: https://dx.doi.org/10.1080/02626668809491275.
47) Egboka BCE, Onyebueke FO. Acute hydrogeological problem Vis-a-Vis planning and management of a developing economy: A case study of Enugu area. *Nigeria Journal of water resources NAH*. 1999;2(1):43–55. Available from: https://www.scrip.org.
48) Akudinobi BEB, Egboka BCE. Aspects of hydrogeological studies of the escarpment regions of southeastern Nigeria. *Water Resources Journal Nigeria Association of Hydrogeology*. 1996;7(12):12–25. Available from: https://scholar.google.com.
49) Vanovermereen RA. Aquifer boundaries explored by geoelectrical measurement of Yemen: A case of equivalence. *Geophysics*. 1989;4(1):38–48. Available from: https://dx.doi.org/10.1190/1.1442575.
50) Batayneh TA. A Hydrogeophysical Model of the Relationship between Geoelectric and Hydraulic Parameters, Central Jordan. *Journal of Water Resource and Protection*. 2009;01(06):400–407. Available from: https://dx.doi.org/10.4236/jwarp.2009.16048.
51) Gemail KS, El-Shishtawy AM, El-Alfy M, Ghoneim MF, El-Bary MHA. Assessment of aquifer vulnerability to industrial waste water using resistivity measurements. A case study, along El-Gharbyia main drain, Nile Delta, Egypt. *Journal of Applied Geophysics*. 2011;75(1):140–150. Available from: https://dx.doi.org/10.1016/j.jappgeo.2011.06.026.
52) Heigold PC, Gilkeson RH, Cartwright K, Reed PC. Aquifer Transmissivity from Surficial Electrical Methods. *Ground Water*. 1979;17:338–345. Available from: https://dx.doi.org/10.1111/j.1745-6584.1979.tb03326.x.
53) Stempvoort DV, Ewert L, Wassenaar L. AVI: A method for groundwater protection mapping in the prairie provinces of Canada. *Prairie Provinces Water Board Report Regina, SK*. 1992;114.
54) Loke MH. Tutorial: 2-D and 3-D electrical imaging surveys. Revised edition ed. and others, editor. 2011. Available from: www.geoelectrical.com.
55) Loke MH. Electrical Imaging Surveys for Environmental and Engineering Studies, A Practical Guide to 2D and 3D Surveys. Workshop held in USM. 1999. Available from: www.terrajp.co.Jp/lokenote.pdf.
56) Mooney HM. Handbook of Engineering geophysics: Electrical resistivity. Minneapolis, Minneasota. 1980.
57) Barker R, Rao TV, Thangarajan M. Delineation of contaminant zone through electrical imaging technique. *Current Science*. 2001;81(3):277–283. Available from: https://www.researchgate.net/2858.
58) Mogaji KA, Adiat K, Oladapo MI. Geoelectric investigation of the Dape area phase III housing estate FCT. *Journal of Earth Science*. 2007;1(2):76–84. Available from: https://www.researchgate.net/publication/265380681.